JOURNAL OF AIRCRAFT
Vol. 42, No. 6, November–December 2005

Engineering Notes

ENGINEERING NOTES are short manuscripts describing new developments or important results of a preliminary nature. These Notes should not exceed 2500 words (where a figure or table counts as 200 words). Following informal review by the Editors, they may be published within a few months of the date of receipt. Style requirements are the same as for regular contributions (see inside back cover).

Dynamic Analysis of Aircraft Landing Impact Using Landing-Region-Based Model

Xiao-Hui Wei* and Hong Nie†
Nanjing University of Aeronautics and Astronautics, Nanjing 210016, China

Nomenclature

A_a = pneumatic area
A_h = hydraulic area
A_o = area of opening in orifice plate
A_p = cross-sectional area of metering pin or rod in plane of orifice
A_0 = net orifice area
C_d = orifice discharge coefficient
d = damping coefficient of supporting damper
F_a = pneumatic force in shock strut
F_C = damping force applied on the floating mass
F_h = hydraulic force in shock strut
F_K = spring force applied on the floating mass
F_S = total axial shock-strut force
F_{Va} = vertical force, applied at axle
F_{Vg} = vertical force, applied to tire at ground
g = gravitational constant
h = bulge height (height of upper surface of floating mass over runway)
K_L = lift factor, L/w
k = stiffness of supporting spring
L = lift force
m, r = constants corresponding to the various regimes of the tire-deflection process
n = polytropic exponent for air-compression process in shock strut
p_{a0} = air pressure in upper chamber of shock strut at zero stroke
p_h = hydraulic pressure in lower chamber of shock strut
r_d = radius of deflected tire
s = shock-strut axial stroke
v_0 = air volume of shock strut at zero stroke
w = total dropping weight
w_1 = weight of upper mass above strut
w_2 = weight of lower mass below strut
w_3 = weight of floating mass
z_1 = vertical displacement of upper mass from position at initial contact
z_2 = vertical displacement of lower mass from position at initial contact
z_3 = vertical displacement of floating mass from position at initial contact
ρ = mass density of hydraulic fluid
δ = deflection of the tire

Received 1 December 2003; revision received 16 September 2004; accepted for publication 23 November 2004.

*Graduate Student, College of Aerospace Engineering; weixiaohuinuaa@hotmail.com.
†Professor, College of Aerospace Engineering; hnie@nuaa.edu.cn.

Introduction

DURING the process of landing, an aircraft is exposed to a short-duration impulsive impact. The landing impact has been recognized as a significant factor in structural fatigue damage, dynamic stress on the aircraft airframe, and crew and passenger discomfort.[1] How to effectively absorb aircraft-landing kinetic energy to attenuate impact loads on aircraft is a problem facing landing gear designers.

With the requirements of increased weight and sink velocity in aircrafts design, the loads on airframes and landing gear increase correspondingly. This problem is especially the case during carrier plane landings on decks[2] and horizontal space shuttle landings.[3]

For the past decades, many efforts have been made to learn the behavior of landing gear during touchdown.[4–10] With this known behavior of landing gear, a number of methods have been developed to attenuate landing impact loads. One of them is to improve the structural type of landing gear or the dynamic characteristics of the shock strut, which is the main component of the landing gear system.[11–14] Another way to attenuate the landing impact loads is to embed a control system into the landing gear system.[15–21]

This article introduces a new conception, named the landing region, to attenuate landing impact loads during touchdown. A landing region is actually a mechanism that is built on a runway. The main contribution of this study is to demonstrate a new way to attenuate landing impact loads. To achieve this goal, a theoretical model for the landing region is developed. With this theoretical model, the landing process is theoretically constructed, and its governing equation is derived. The performance of simulated landing gear systems landing on this landing region is theoretically evaluated during touchdown. Studies have also been made to determine the effects of variations in some landing region parameters. The authors expect that such a landing region can be realized to attenuate the landing impact loads of carrier-based aircraft during the process of landing on the decks of aircraft carriers in the future.

Modeling of the Landing Gear and Landing Region

Landing Gear

Dynamics of landing gear systems follows the dynamic model of Ref. 5. It is assumed in the analysis that the landing gear is attached to a rigid mass that has freedom only in vertical translation. The gear is assumed to be infinitely rigid in bending. The combination of airplane and landing gear considered therefore constitutes a system having two degrees of freedom, as defined by the vertical displacement of the upper mass and the vertical displacement of the lower or unsprung mass, as shown in Fig. 1a. Figure 1b shows a schematic representation of a typical oleopneumatic shock strut.

From consideration of the forces and pressures acting in the shockstrut, it can be readily seen from Fig. 1b that the total axial force due to hydraulic resistance and air compression can be expressed by

$$F_S = F_h + F_a \tag{1}$$

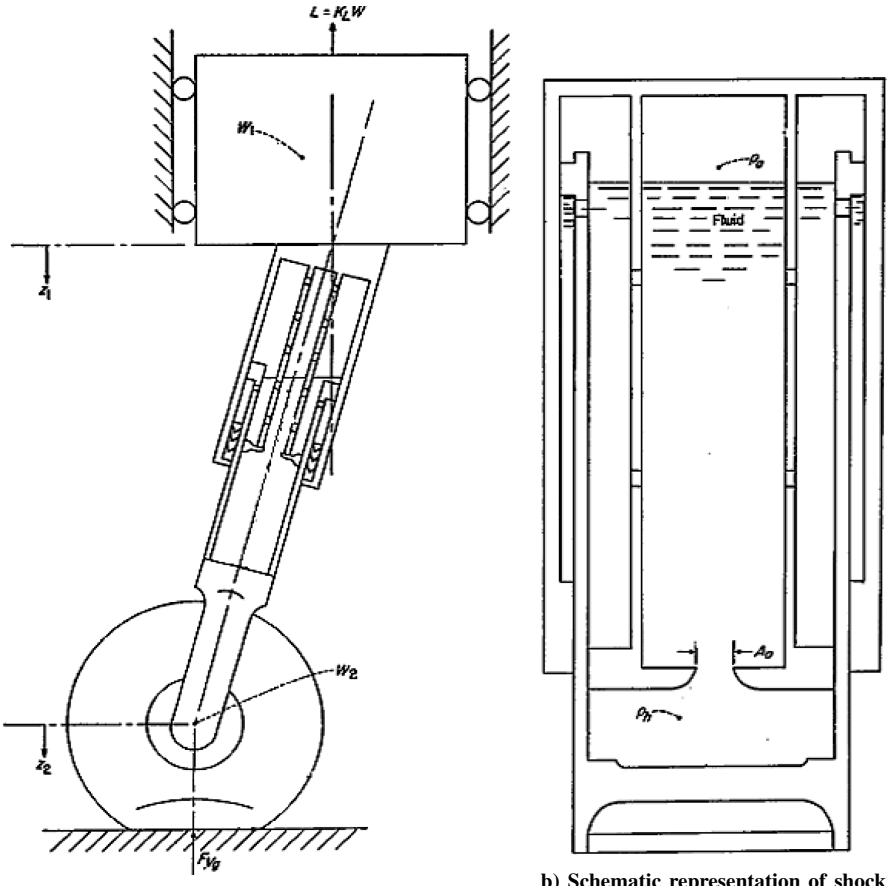

a) System with two degrees of freedom

b) Schematic representation of shock strut

Fig. 1 Freedom of landing gear system and schematic representation of its shock strut.

where

$$F_h = \frac{\dot{s}}{|\dot{s}|}\frac{\rho A_h^3}{2\,(C_d A_0)^2}\dot{s}^2 \tag{2}$$

$$F_a = p_{a0}A_a\left(\frac{v_0}{v_0 - A_a s}\right)^n \tag{3}$$

If the exponential characteristics of the tire without hysteresis are considered, tire force is given by

$$F_{\mathrm{Vg}} = m\delta^r \tag{4}$$

In the case of severe impacts where tire bottoming occurs, new values of m and r are employed in the tire-bottoming regime.

Landing Region

A landing region is actually a mechanical system that is built on a runway. The landing region comprises three major parts: floating mass, supporting spring, and supporting damper. In the first approximation, the floating mass is considered as a rigid mass that has freedom only in vertical translation, the supporting spring is linear, the supporting damper is linear viscous, and the floating mass is locked at the time when the upper surface of the floating mass level is down to the runway surface. Figure 2 shows the schematic representation of this system and the balance of forces and reactions for it.

According to the assumptions mentioned above, spring force anddamping force are given by

$$F_K = kz_3, \qquad F_C = d\dot{z}_3 \tag{5}$$

Equations of motion

The motion of landing impact can be treated as having three phases. The first phase is the time interval from the instant of contact to the beginning of shock-strut deflection; the second phase is the time interval from the beginning of shock-strut deflection to the instant at which the floating mass is locked; the third phase is the time interval from the instant at which the floating mass is locked to the end of the impact.

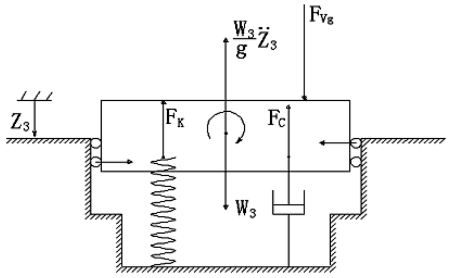

Fig. 2 Sketch map of landing region.

The First Phase

Because $\ddot{z}_1 = \ddot{z}_2 = \ddot{z}$ during this first phase of the impact, the system may be considered to have two degrees of freedom, which are made up of freedom z and freedom z_3. Thus, the overall dynamic equilibrium of the landing gear is given by

$$F_{\mathrm{Vg}}(z - z_3) = -(w/g)\ddot{z} - w(K_L - 1) \tag{6}$$

The governing equation of the floating mass is given by

$$w_3 + F_{\mathrm{Vg}}(z - z_3) - F_K - F_C = (w_3/g)\ddot{z}_3 \tag{7}$$

The Second Phase

Because the shock strut begins to deflect during this second phase of impact, the system may be considered to have three degrees of freedom, which are made up of freedom z_1, freedom z_2, and freedom z_3. The equation of motion for the upper mass is

$$F_S + L - w_1 = -(w_1/g)\ddot{z}_1 \tag{8}$$

The equation of motion for the lower mass is

$$F_S + w_2 - F_{\mathrm{Vg}}(z_2 - z_3) = (w_2/g)\ddot{z}_2 \tag{9}$$

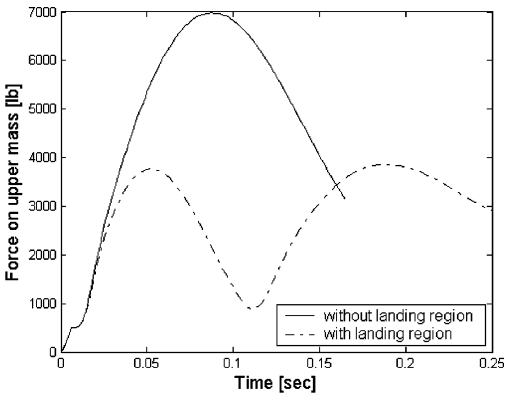

a) Time histories of force on upper mass

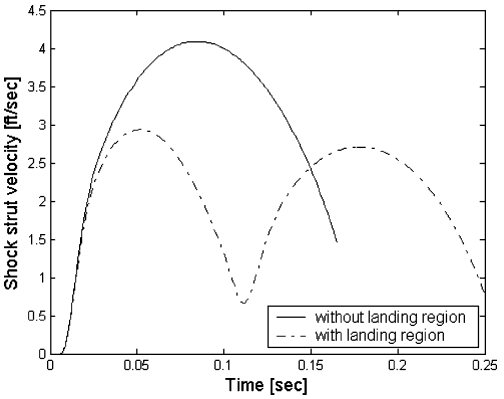

c) Time histories of shock strut velocity

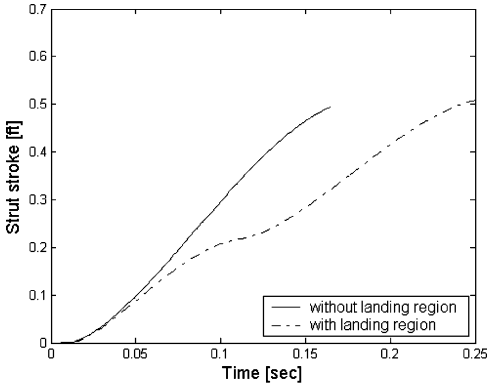

b) Time histories of shock strut stroke

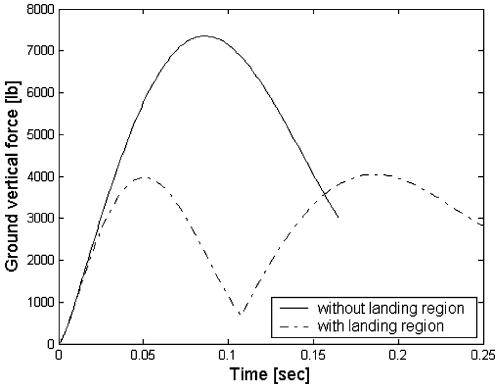

d) Time histories of ground vertical force

Fig. 3 Comparison between the results from this new model and those from the conventional model.

The equation of motion for the floating mass is

$$w_3 + F_{\mathrm{Vg}}(z_2 - z_3) - F_K - F_C = (w_3/g)\ddot{z}_3 \tag{10}$$

The Third Phase

Because the floating mass is locked during this third phase of impact, the system may be considered to have two degrees of freedom, freedom $z_1$and freedom z_2. The equation of motion for the upper mass is the same as Eq. (6). The equation of motion for the lower mass is

$$F_S + w_2 - F_{\mathrm{Vg}}(z_2 - h) = (w_2/g)\ddot{z}_2 \tag{11}$$

Solution of Equations of Motion

The use of the tire-deflection characteristics in the calculations neglected hysteresis of the tire, except in the case of severe impacts where tire bottoming occurs. The effects of drag loads were neglected in the calculations. The validity of the dynamic model without a landing region was verified in Ref. 5. A dynamic model of this new system was built up based on the dynamic model without a landing region. Also, in these calculations, the discharge coefficient for the orifice and the polytropic exponent for the air-compression process were assumed to have constant values throughout the impact. The discharge coefficient was assumed to be equal to 0.9 and the polytropic exponent was assumed to be equal to 1.12. In view of the fact that the landing gear was mounted in a vertical position and drag loads were absent in the tests mentioned in Ref. 5, friction forces in the shock strut were assumed to be negligible in the calculations. Because the weight was fully balanced by lift forces in the tests, the lift factor K_L was taken equal to 1.0.

Normal Impact

Normal impact refers to a vertical velocity of 8.86 fps at the instant of ground contact. Figure 3 presents a comparison of calculated results based on this new model with calculated results based on the model without a landing region.

Calculated time history of total force on the upper mass is compared with that calculated from the model without a landing region in Fig. 3a. Similar comparisons for the strut stroke, strut telescoping velocity, and ground vertical force are presented in Figs. 3b, 3c, and 3d, respectively. As can be seen from Fig. 3a, when the landing region is introduced, there are two maximum values during the process of landing impact, and the maximum value of the force on the upper mass is reduced 45%. The two separate peaks are due to the introduction of the landing region. When the forces on the upper mass reach a certain value, namely the first peak, the tires cannot be compressed any more and rebound gradually. Then the forces decrease gradually until the floating mass is locked. When the floating mass is locked, the tires are compressed again. Then the forces increase gradually until the second peak is reached. Similar circumstances occur in shock strut velocity and ground vertical force, and the maximum values of these are reduced 28% and 45%, respectively.

Severe Impact

Severe impact refers to a vertical velocity of 11.63 fps at the instant of ground contact. For the model without landing region, tire bottoming occurs in this case. Figure 4 presents a comparison of calculated results based on this new model with calculated results based on the model without a landing region.

Calculated time history of total force on upper mass is compared with that calculated from the model without a landing region in Fig. 4a. Similar comparisons for the strut stroke, strut telescoping velocity, and ground vertical force are presented in Figs. 4b, 4c, and 4d, respectively. As can be seen from Fig. 4a, the maximum value of force on upper mass is reduced 49.0%, and tire bottoming does not appear.

Parameter Studies

In the preceding section, comparisons of calculated results of this new model with calculated results without a landing region shows that, the impact loads have been reduced significantly. In view of the fact that the parameters of the landing region are not readily known currently, calculations have been made to evaluate the effect

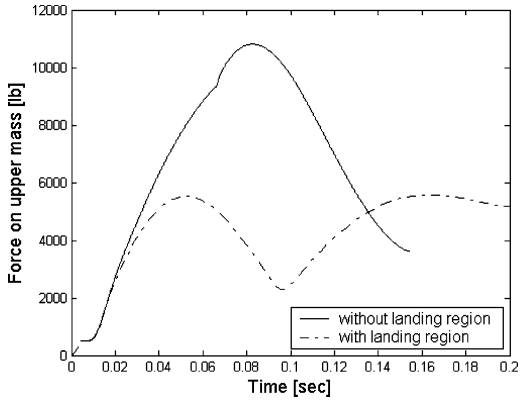

a) Time histories of force on upper mass

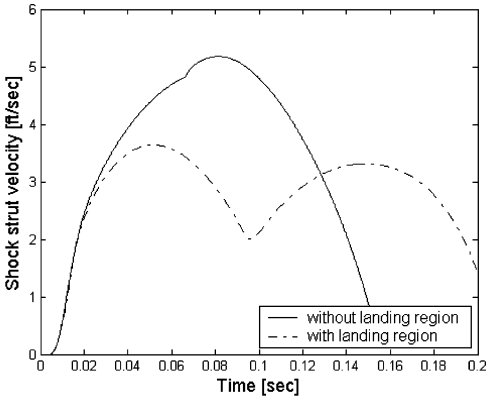

c) Time histories of shock strut velocity

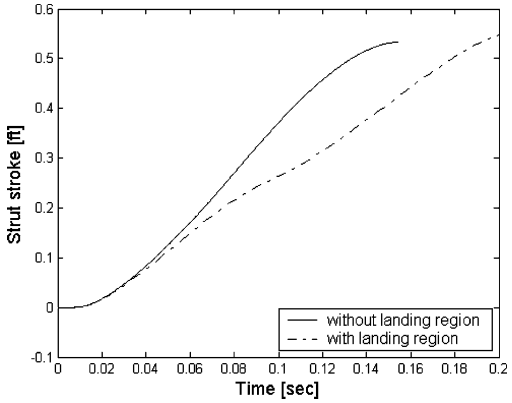

b) Time histories of shock strut stroke

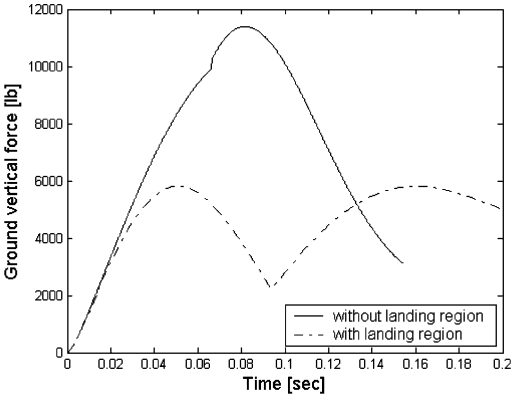

d) Time histories of ground vertical force

Fig. 4 Comparison between the results from this new model and those from the conventional model.

of these parameters on the landing gear behavior. The results of these calculations are all for normal impact.

The solutions presented are for the same set of initial conditions as for the normal impact without tire bottoming, previously considered, and are based on exponential tire-force-deflection characteristics that neglect hystersis.

Effect of the Stiffness of Supporting Spring

Figure 5 presents comparisons of calculated results for a range of values of the stiffness of supporting spring k between 500 lbf, ft and infinite. In fact, for stiffness of supporting spring k larger than 15,172 lbf, ft, the floating mass cannot sink down to the surface of the runway. Under the current assumed conditions,the stiffness of the supporting spring k should not be larger than 15,172 lbf, ft.

The calculations show that an increase in the stiffness of the supporting spring results in a small increase in the first maximum value of the force on the upper mass, as well as a decrease in the second maximum value of the force on the upper mass. This variation is to be expected because the greater stiffness of the supporting spring results in greater spring force. Thus, the first maximum value of the force on the upper mass increases and the spring deposits more energy before the floating mass is locked, and then the second maximum value of the force on the upper mass decreases. Similar circumstances occur for strut velocity and ground vertical force.

Effect of the Damping Coefficient of Supporting Damper

Figure 6 presents comparisons of calculated results for a range of values of the damping coefficient of supporting damper d between no damping and 1000 lbf·s/ft.

The calculations show that an increase in the damping coefficient of the supporting damper results in an increase in the first maximum value of the force on the upper mass, as well as a great decrease in the second maximum value of the force on the upper mass. This variation is to be expected because a greater damping coefficient of the supporting damper results in a greater damper resistance force. Thus, the first maximum value of the force on the upper mass increases and the damper dissipates more energy, and then the second maximum value of the force on the upper mass decreases. Similar circumstances occur for strut velocity and ground vertical force.

Effect of the Weight of Floating Mass

Figure 7 presents comparisons of calculated results for a range of values of the weight of the floating mass w_3 between 635.5 and 2542 lb.

The calculations show that an increase in the weight of the floating mass results in an approximately proportional increase in the first maximum value of the force on the upper mass, as well as an approximately proportional decrease in the second maximum value of the force on the upper mass. This variation is to be expected because the impact force is related to the ratio of the weight of the floating mass and the landing weight. The greater the ratio is, the greater the first maximum value will be, and more energy the landing region will dissipate during the first peak.Therefore, the second peak is reduced correspondingly. Similar circumstances occur for strut velocity and ground vertical force.

Effect of the Bulge Height

Figure 8 presents comparisons of calculated results for a range of values of the bulge height h between 0.0 and 0.5 ft.

The calculations show that a decrease in the bulge height results in no effect on the first maximum value of the force on the upper mass and a significant increase in the second maximum value of the force on the upper mass. This variation is to be expected because the first maximum value of the force on the upper mass is completely determined by the weight of the floating mass, the damping coefficient of the supporting damper, and the stiffness of the supporting spring. The less the height is, the less the effect on landing behavior will be. Similar circumstances occur for strut velocity and ground vertical force.

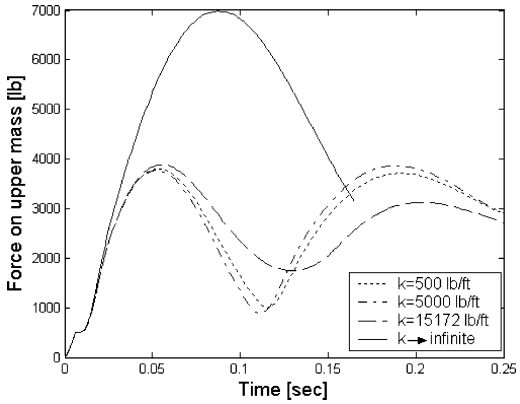

a) Time histories of force on upper mass

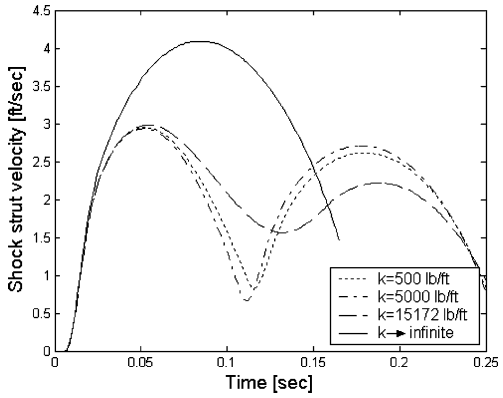

c) Time histories of shock strut velocity

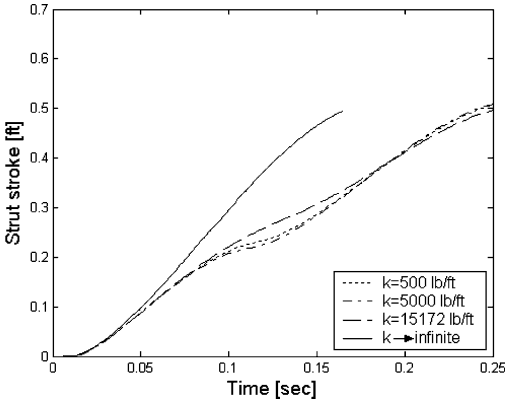

b) Time histories of shock strut stroke

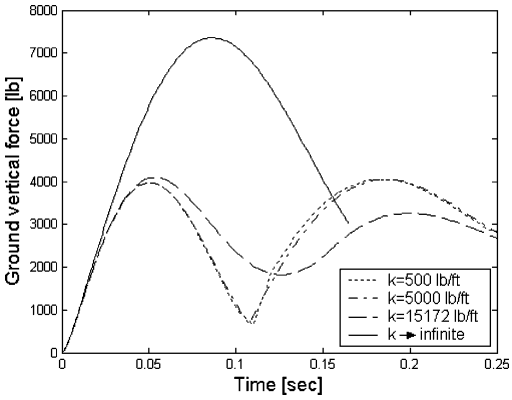

d) Time histories of ground vertical force

Fig. 5 Effect of stiffness of supporting spring on the behavior of landing gear impact.

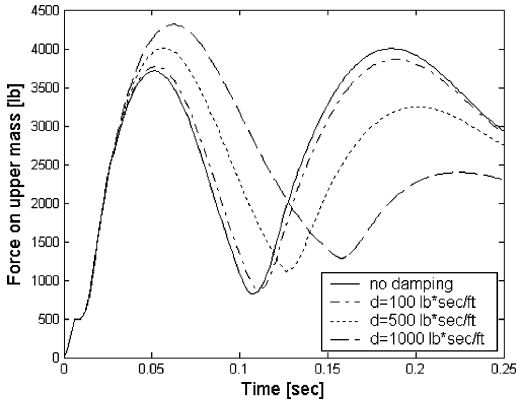

a) Time histories of force on upper mass

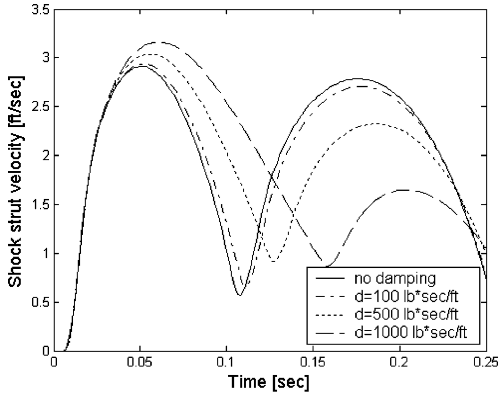

c) Time histories of shock strut velocity

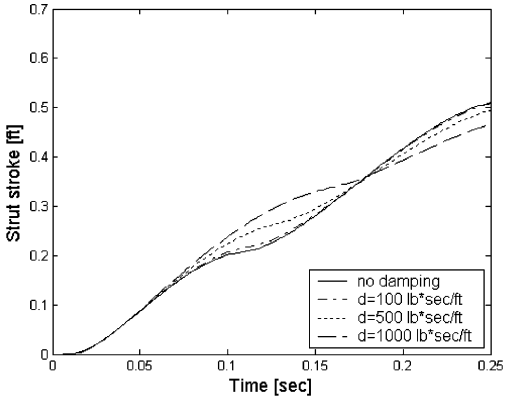

b) Time histories of shock strut stroke

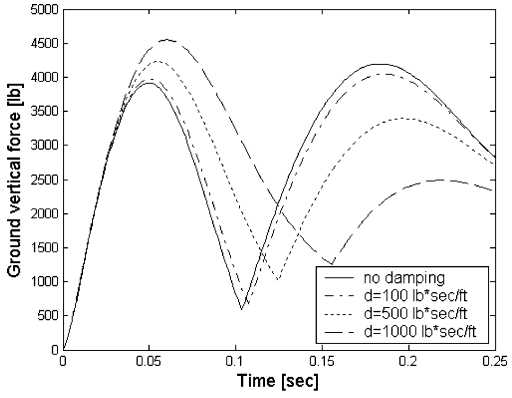

d) Time histories of ground vertical force

Fig. 6 Effect of damping coefficient of supporting damper on behavior of landing gear impact.

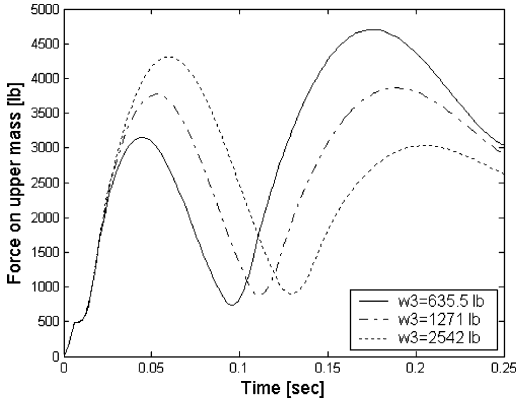

a) Time histories of force on upper mass

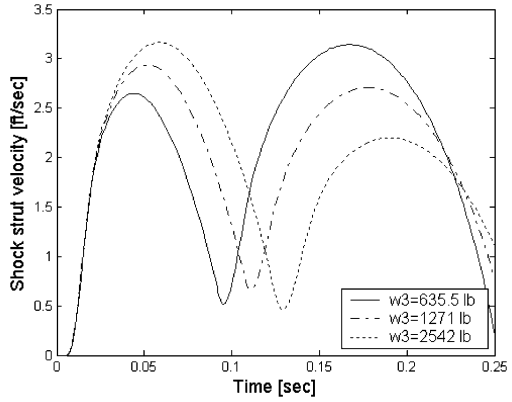

c) Time histories of shock strut velocity

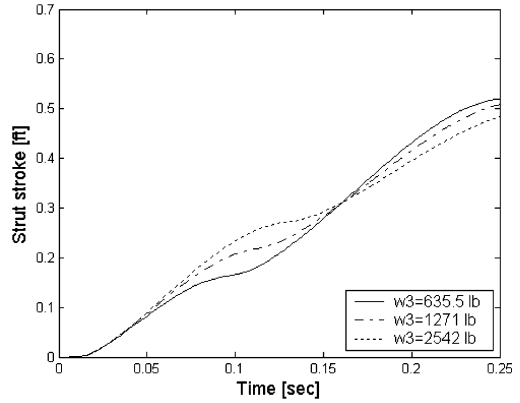

b) Time histories of shock strut stroke

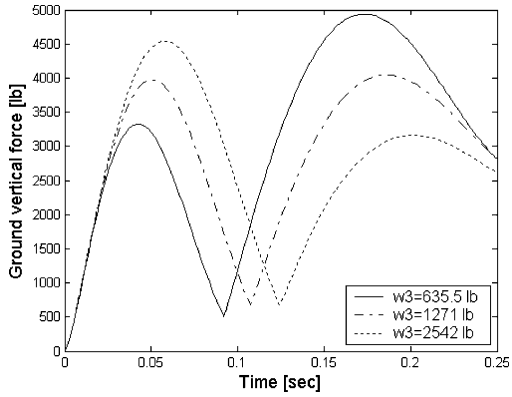

d) Time histories of ground vertical force

Fig. 7 Effect of floating mass on the behavior of landing gear impact.

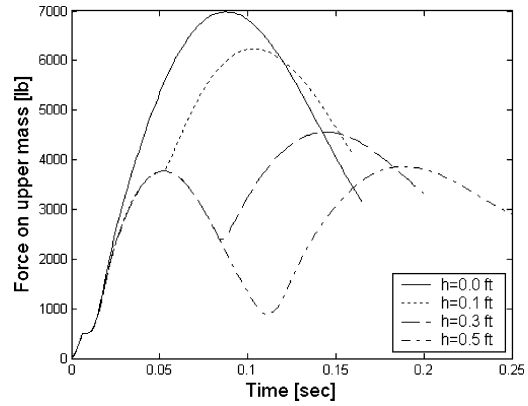

a) Time histories of force on upper mass

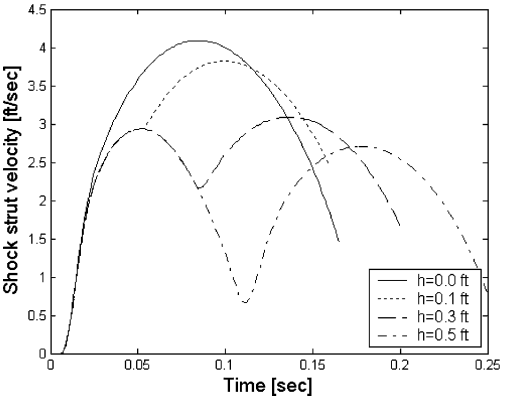

c) Time histories of shock strut velocity

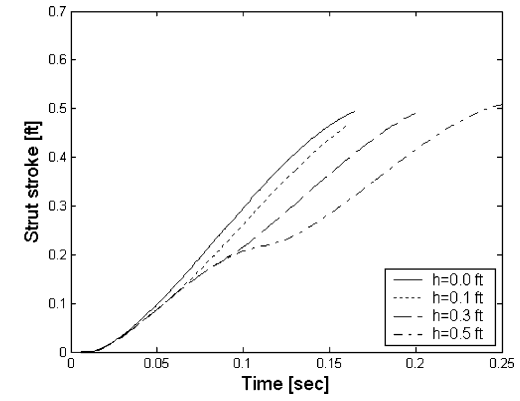

b) Time histories of shock strut stroke

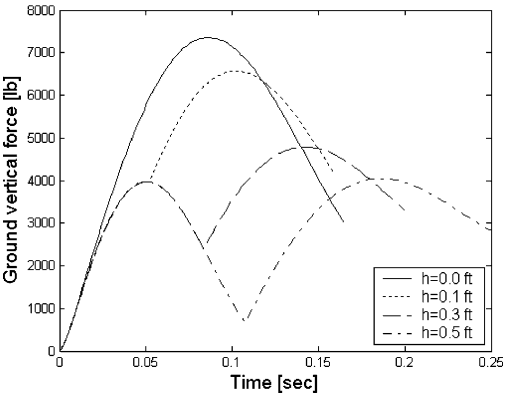

d) Time histories of ground vertical force

Fig. 8 Effect of bulge height on behavior of landing gear impact.

Conclusion

In this paper, we have introduced a new conception of a landing region and have analyzed the behavior of landing impact based on the model with a landing region. It is found that the force on the upper mass is reduced 44.7% and 49.0% when a normal impact speed of 8.86 fps and a severe impact speed of 11.63 fps are considered, respectively.

In addition, we have studied the effect of some landing region parameters on the behavior of landing impact. The study of the effects of variations in the stiffness of the supporting spring indicate that the stiffness of the supporting spring has only a limited effect on the behavior of landing impact. An increase in the stiffness of the supporting spring leads to a minor increase in the first maximum value and a minor decrease in the second maximum value. The study of the effects of variations in the damping coefficient of the supporting damper indicate that the damping coefficient of the supporting damper also has a limited effect on the behavior of landing impact. The effect of the damping coefficient of the supporting damper on the landing impact is similar to the effect of the stiffness of the supporting spring. The study of the effects of the weight of the floating mass indicates that the weight of the floating mass has an important effect on the behavior of landing impact. An increase of the weight the floating mass will result in an approximately proportional increase of the first maximum value and an approximately proportional decrease of the second maximum value.The study of the effects of the bulge height of the landing region indicates that the bulge height has the most significant effect on the maximum value of impact force. Obviously, if the bulge height equals zero, the behavior of landing impact will be the same in the results without a landing region.

All of the above conclusions must be treated as tentative because the actual landing region is not established yet. In addition, the behavior of all components of the landing region is idealized. Analysis based on actual conditions will be the aim of further research.

Acknowledgments

The authors acknowledge research support under the National Natural Science Foundation of China under Grant 10072025.

References

[1]Choi, Y. T., and Wereley, N. M., "Vibration Control of a Landing Gear System Featuring Electrorheological/Magnetorheological Fluids," *Journal of Aircraft*, Vol. 40, No. 3, 2003, pp. 432–439.

[2]Wang, M. H., and Zhao, B., "Investigation for the Take-Off and Landing Dynamic Behavior of Carrier Based Aircraft," *Chinese Aircraft Design*, Vol. 1, March 1997, pp. 21–33.

[3]Nebylov, A. V., and Tomita, N., "Control Aspects of Aerospace Plane Docking with Ekranoplane for Water Landing," *Proceeding of Automatic Control in Aerospace*, International Federation of Automatic Control, Seoul, South Korea, 1998, pp. 379–384.

[4]Flugge, W., "Landing-Gear Impact," NACA TN 2743, 1952.

[5]Milwitzky, B., and Cook, F. E., "Analysis of Landing-Gear Behavior," NACA Report 1154, 1953.

[6]Deakins, R. R., and Blackburn, C. L., "Simulation of High Sink Speed Landing Gear," SAE Paper 650845, Society of Automotive Engineering, 1965.

[7]Maksimova, T. I., "Vibrations of the Principal Struts of a Landing Gear During Landing," *Theory and Practice of Designing Passenger Aircraft*, A77-27126 11-01, Moscow, Izdatel stvo Nauka, 1976, pp. 345–350.

[8]Abrahan, B., "Dynamic Analysis of Landing Impact," IAITIC-82-1006, PB83-188383, 1982.

[9]Yadov, D., and Ramamoorthy, R. P., "Nonlinear Landing Gear Behavior at Touchdown," *Journal of Dynamic Systems, Measurement, and Control*, Vol. 113, Dec. 1991, pp. 677–683.

[10]Kothari, S. S., Ananthasayanam, M. R., and Rajaiah, K., "Analysis of Dynamical Behavior of an Aircraft at Touchdown," *Proceeding of the 31st Aircraft Symposium*, Vol. 31, Japan Science and Technical Corp., Tokyo, 1993, pp. 82–85.

[11]Currey, N. S., *Aircraft Landing Gear Design: Principles and Practices*, AIAA Education Series, AIAA, Washington, DC, 1988, pp. 1–67.

[12]Nie, H., and Qiao, X., "Dynamic Behavior Analysis for Landing Gear with Different Types of Dual-Chamber Shock Struts," *Chinese Journal of Aeronautics*, Vol. 4, May 1991, pp. 235–244.

[13]Nie, H., and Lim, K. H., "Optimal Design for Initial Pressures of Dual-Chamber Shock Absorbers in Landing Gears," *Proceedings of the KSME International Sessions on Dynamics, Systems and Design*, Inchon, South Korea, Nov. 1996, pp. 181–188.

[14]Pink, J., "Landing Gear Structural Integrity," *Aerospace Engineering*, Vol. 16, No. 3, 1996, pp. 13–16.

[15]Bender, E. K., and Beiber, M., "A Feasibility Study of Active Landing Gear," AFFDL TR-70-126, U.S. Air Force Flight Dynamics Lab., Wright Patterson Air Force Base, OH, July 1971.

[16]Mc Gehee, J. R., and Carden, H. D., "A Mathematical Model of an Active Control Landing Gear for Load Control During Impact and Roll-Out," NASA TN D-8080, 1976.

[17]Ross, I., and Edson, R., "An Electronic Control for an Electro-hydraulic Active Control Landing Gear for the F-4Aircraft," NASA CR 3552, April 1982.

[18]Ross, I., and Edson, R., "Application of Active Control Landing Gear Technology to the A-10 Aircraft," NASA CR 166104, June 1983.

[19]Krueger, W., Besselink, I., Cowling, D., Doan, D. B., Kortuem, W., and Krabacher, W., "Aircraft Landing Gear Dynamics: Simulation and Control," *Vehicle System Dynamics*, Vol. 28, Nos. 2–3, 1997, pp. 119–158.

[20]Berg, C. D., and Wellstead, P. E., "The Application of a Smart Landing Gear Oleo Incorporating Electrothelogical Fluid," *Journal of Intelligent Material Systems and Structures*, Vol. 9, No. 8, 1998, pp. 592–600.

[21]Kwak, S. K., Washington, G., and Yedavalli, R. K., "Acceleration Feedback-Based Active and Passive Vibration Control of Landing Gear Components," *Journal of Aerospace Engineering*, Vol. 15, No. 1, 2002, pp. 1–9.